Resources, Conservation & Recycling 178 (2022) 106087

Contents lists available at ScienceDirect

Resources, Conservation & Recycling

journal homepage: www.elsevier.com/locate/resconrec

Assessing the impact of electricity consumption on water resources in the U.S.

Li Chen, Aaron P Wemhoff *

Department of Mechanical Engineering, Villanova University, 800 Lancaster Ave., Villanova, PA, 19085, USA

ARTICLE INFO

Keywords:
Electricity consumption
Indirect water use
Water scarcity footprint (WSF)
Input-output model
Available water remaining (AWARE)
Scarce water index (SWI)

ABSTRACT

Electricity generation heavily relies on water. Growing electricity demand globally inevitably leads to water availability concerns. This study proposes a means to quantify the indirect water usage embodied in electricity and assesses the holistic impact of water consumption on available water resources. First, the energy water intensity factor (EWIF), which quantifies the amount of water used to produce energy, is updated at the contiguous U.S. balancing authority (BA) level and on an end user basis to account for electricity trades using an input-output model. Further, the scarce water index (SWI), or volume of scarce water embodied per kWh electricity consumed, is proposed to predict electricity consuming facility water stress impact as the water scarcity footprint (WSF). A case study of U.S. data centers is presented to demonstrate the use of these metrics. Results show that WSF is region-dependent, and the burden of regional water scarcity extends beyond region boundaries.

1. Introduction

The U.S. consumed 3.8 trillion kWh of electricity in 2020 and approximately 34.8% of U.S. total electricity is consumed by the commercial sector (US EIA, 2021). According to U.S. Department of Energy (DOE), the average power density for a commercial building is 242.2 kWh/m^2, which could be much higher for electricity intensive facilities such as data centers, raising concerns about the environmental burden associated with indirect water consumption.

Previous studies quantified water use in the construction phase (Bardhan and Choudhuri, 2016; Crawford and Pullen, 2011; Meng et al., 2014) and operational phase (Arpke and Hutzler, 2005; Crawford and Pullen, 2011; Proença and Ghisi, 2010; Willis et al., 2013) of a building's lifecycle. The indirect water consumption associated with virtual water transfers should be included to better understand building water use. Many researchers have investigated the virtual water transfers embedded in domestic supply chains, the food-energy-nexus, and the electric grid at global or national scales (Bartos and Chester, 2014; Chapagain and Hoekstra, 2008; Chen and Wemhoff, 2021b; Cohen and Ramaswami, 2014; Dang et al., 2015; Garcia et al., 2020; Liao et al., 2018; Mubako and Lant, 2013; Zhang et al., 2017; Zhang et al., 2016). (Chini et al., 2018) analyzed the virtual water flows of the U.S. electric grid and the changes in the water transfer network structure from 2010 to 2016. Their analysis at the power control area (PCA) level adapted the network approach first proposed by Kodra et al. (Kodra et al., 2015) with water consumption data associated with electricity generation from the Emissions & Generation Resource Integrated Database (eGRID) (US EPA, 2015a). However, their study can be improved in two ways: first, by applying a quasi-input-output (QIO) model by Qu et al. (Qu et al., 2017) to improve the accuracy of the network approach, and also by addressing inaccuracies in water consumption data for power generation since eGRID only collects and reports data for power plants that exceed certain power capacity, which also ignores some important water consuming processes that contributes to the overall water footprint (i.e., the processes upstream of the point of generation (PoG)) (US EPA, 2015a). Incorporating the water consumption associated with power generation avoids this issue. The water required for electricity generation has been extensively investigated (Macknick et al., 2012; Meng et al., 2020; Peer et al., 2019; Peer and Sanders, 2018; Sanders, 2014; Wang et al., 2017) and the energy water intensity factor (EWIF), which quantifies the amount of water used to produce energy, is widely used in water-energy nexus research. In particular, Peer et al. (Peer et al., 2019) estimated the operational life cycle water consumption for electricity generation at the eGRID subregion level. However, the electricity transmissions among regions were not considered, and water is often virtually transferred within electricity flows.

* Corresponding author .
E-mail address: aaron.wemhoff@villanova.edu (A.P. Wemhoff).

https://doi.org/10.1016/j.resconrec.2021.106087
Received 24 August 2021; Received in revised form 24 November 2021; Accepted 25 November 2021
Available online 5 December 2021

This study therefore improves predictions of electricity consuming facility indirect water use by estimating EWIF values at the U.S. balancing authority (BA) level. BAs are metered boundaries for power generation and transmission within the contiguous U.S. The predicted EWIF values are from an electricity consumer's point of view and incorporate power generation location, technology, and virtual water transfers. International electricity transfers with Canada and Mexico are included, and the QIO model is implemented to achieve more accurate predictions (Qu et al., 2017).

Furthermore, this study proposes a means to quantify the holistic impact of both direct and indirect water consumption on regional water availability, which is captured as the water scarcity footprint (WSF) per ISO standard 14,046 (ISO 14046:2014). WSF is defined as the product of the volume of water consumed and a water scarcity indicator. Many studies have examined regional water scarcity, and numerous indicators exist (Boulay et al., 2018; Jones and van Vliet, 2018; Lee et al., 2018; Liu et al., 2017; Rijsberman, 2006; Schyns et al., 2015). Notably, Boulay et al. (Boulay et al., 2018) developed an Available Water Remaining (AWARE) method that is now recommended for water scarcity footprint calculations by the United Nations Environment Life Cycle Initiative (Frischknecht et al., 2016). Therefore, the U.S. county level water scarcity indicator, AWARE-US CF, derived by Lee et al. (Lee et al., 2019) by adapting the AWARE approach, is incorporated in this study for WSF quantification. There has been growing interest in the WSF metric since the same amount of water consumption in electricity exporting regions with different water scarcities can result in different impacts on regional water resources. Furthermore, WSF predictions unveil different water footprints from energy demand in importing regions due to different levels of vulnerability (Liao et al., 2020; Ridoutt and Pfister, 2010; Rushforth and Ruddell, 2016; Zhao et al., 2018; Zheng et al., 2016). However, studies that quantify WSF in the energy sector are rare. Xie et al. (Xie et al., 2020) predicted the WSF of electricity generation for China's provinces and concluded that power generation WSF has significant regional variability. Additionally, Liao et al. (Liao et al., 2020) compared the WSF of energy demand for six megacities in China that highlights the impact of energy demand extend beyond city boundaries.

This study builds upon previous research by extending the water stress impact analysis to include direct and indirect water use by all electricity consuming facilities in the U.S. using the AWARE method. The water stress impact is evaluated as the WSF and a new water sustainability metric, the scarce water index (SWI), which measures the volume of scarce water embodied per kWh of electricity consumed, is proposed to achieve this goal.

2. Methods

Assessing facility water usage and its impacts on water availability requires four steps, as shown in Fig. 1:

1 Measure the direct water consumption.
2 Determine the water required for power generation by evaluating EWIF for different power generation technologies in electricity exporting regions. Measure the electricity generation since water use for power generation can be obtained once EWIF and electricity generation are known.
3 Consider the virtual water transfers associated with electricity transmissions, which could significantly alter the regional EWIF values.
4 Calculate WSF by incorporating the AWARE approach and the SWI.

In this study, the EWIF is derived for different locations by following power generation from each source in each region's electricity generation portfolio. The environmentally extended input-output (EEIO) model, inspired by economic input-output theory, (Qu et al., 2017) is used to trace the electricity interregional transfers and their associated water relocation, enabling the calculation of SWI. The WSF is then calculated using the SWI to analyze the impacts of electricity consuming facility water use on regional water scarcity. The following sections detail the approach and the data used for evaluating the indirect water use and regional water stress associated with electricity consuming facility.

2.1. Assessing the impacts of water consumption

Several regions in the U.S. are experiencing more frequent and longer durations of droughts due to climate change (Jones and van Vliet, 2018), so assessing an electricity consumer's regional water stress is important. The WSF, recommended in ISO 14046 (ISO 14046:2014), is the metric that quantifies the potential environmental impacts related to water. By its definition, WSF can be calculated using

$$\text{WSF} = \text{Water Consumption}\left[\text{m}^3\right] \times \text{Water Scarcity Indicator} \tag{1}$$

The WSF represents the volume of water consumption that also accounts for water availability. It enables the comparison of water consumption in different regions. Lee et al. (Lee et al., 2019) adapted the AWARE approach and developed the U.S. model at a refined spatial scale (i.e., the county-level) to quantify the water scarcity and impacts of water consumption in different regions within the contiguous U.S. Their characterization factor (AWARE-US CF) (Boulay et al., 2018; Lee et al.,

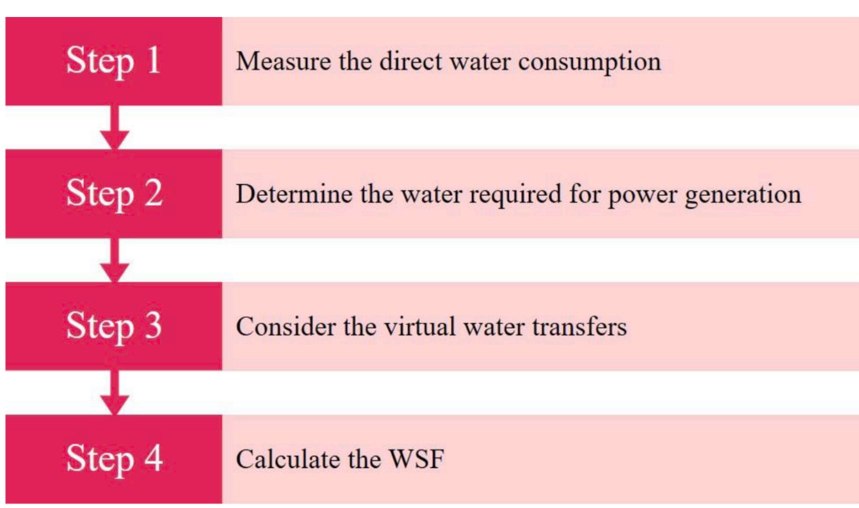

Fig. 1. Steps required to assess the impacts of water consumption on regional water availability.

2019) compares regional available water to a reference value:

$$\mathrm{AWARE-USCF} = \frac{AMD_{ref}}{AMD} \tag{2}$$

where *AMD* indicates water availability minus demand, and is the reference value of *AMD* that is estimated as the weighted average of all regions (Lee et al., 2019). By its definition, AWARE-US CF is bounded between 0.1 to 100, and high AWARE-US CF values represent water scarce regions. Therefore, large WSF values, indicating a more intense relationship between water consumption and regional water availability, can either be caused by high water consumption or severe water scarcity.

The WSF metric should include the water stress associated with both on-site water use as well that embodied in electricity, which is especially important for facilities with large electricity consumption. Eqn. (1) indicates that an accurate WSF prediction requires quantifying the contribution of both flows. Therefore, the WSF calculation proposed here considers both direct and indirect water consumption:

$$\mathrm{WSF} = (\mathrm{AWARE-US\ CF})(W_{site}) + (\mathrm{SWI})(P_{site}) \tag{3}$$

where W_{site} and P_{site} are the site water and power consumption, respectively. The AWARE-US CF and SWI here are specific to the facility location, where SWI quantifies the impact of electricity consumption on regional water availability. Thus, the WSF of a facility with known power load and on-site water consumption can easily be calculated based on the location-specific factors AWARE-US CF and SWI. Eqn. (3) shows that theoretically an intensive water consuming facility with a large direct water consumption could result in a lower WSF than a facility requiring less direct water consumption if P_{site} and SWI are large. Here, AWARE-US CF and SWI are specific to the county and BA levels, respectively, since AWARE-US CF is highly location dependent and SWI is based on regional electricity flows.

2.2. Measuring water consumption and efficiency

Peer et al. (Peer et al., 2019) presented the regional water consumption and water intensity factor for the entire power grid in the U.S. by analyzing the life cycle water consumption from fuel extraction through conversion for each power generation technology and site. The intensity factors were aggregated to the eGRID subregions classified by the U.S. Environmental Protection Agency (US EPA) (US EPA, 2015a).

This study builds upon Peer et al.'s work and extends the water intensity factors to the U.S. BA level. This extension is necessary because data on detailed power generation, consumption, imports, and exports are required by the EEIO model, and completed electricity trades data are only currently available at the BA-level. In this study, daily electricity data are collected from the hourly electric grid monitoring system developed by the U.S. Energy Information Administration (EIA) and cleaned over the entire 2019 calendar year (Real-Time Operating Grid, 2020).

The water intensity factors derived by Peer et al. (Peer et al., 2019), denoted as EWIF'$_S$ here (the subscript *s* indicates subregions, and the prime indicates the exclusion of electricity transfers) are shown in Fig. 2 (a). Their results indicate that eGRID subregional EWIF'$_S$ values vary from 0.63 to 9.20 L/kWh with an average of 1.81 L/kWh and a standard deviation of 1.58 L/kWh. Since detailed electricity transfer data is only available at the BA-level, then it is necessary to translate the energy intensity factors from the subregion-level (EWIF'$_S$) to the BA-level (EWIF'$_B$) before applying the EEIO model to track the electricity transmissions within the electric grid. First, every county in the contiguous U. S. is assigned to one subregion and one BA. The geographic centroids of counties are used when assigning counties to subregions and BAs because eGRID subregion boundaries and BA boundaries are approximate with no rigid geographical features. In this study, eGRID subregion boundaries are retrieved from the EPA (US EPA, 2015b), and BA boundaries are taken from Homeland Infrastructure Foundation-Level Data (HIFLD) as shown in Fig. 2(a) and Fig. 2(b), respectively (HIFLD Open Data, 2020). Then, assuming that counties within the same eGRID subregion have the same EWIF for a given fuel type, the power generation weighted BA-level EWIF (i.e., EWIF'$_B$) is

$$\mathrm{EWIF}'_{\mathrm{B},i} = \sum_{j=1}^{n_i} \sum_{k=1}^{N_j} \mathrm{EWIF}'_{\mathrm{S},k} \frac{G_{ijk}}{\sum_{j=1}^{n_i} \sum_{k=1}^{N_j} G_{ijk}} \tag{4}$$

where county j is one of n_i counties associated with BA i. The power generation rate and subregion-based, fuel-specific EWIF associated with power generation source k in county j is G_{ijk} and $\mathrm{EWIF}'_{\mathrm{S},k}$, respectively. Finally, N_j is the number of different power generation sources in county j. The power plant data published by EIA in 2020 for all power plants operating with a combined nameplate capacity of 1 MW or more is used here (*Maps - EIA*, 2020).

The prediction of SWI and consumptive EWIF values that incorporate electricity exchanges requires a predictive model of flows in the electric grid. Qu et al. (Qu et al., 2017) first proposed the QIO model, which is an EEIO model that uses a network approach to evaluate the embodied carbon emissions from purchased electricity. The idea can also be applied to track the embodied water consumption in the power grid. In this model, each region is represented as a node that connects to other nodes. Each node can either be an importer, an exporter or both. The electricity interchanges of each node (i) must be conserved, so

$$G_i + \sum_{j=1}^{n} E_{ji} = C_i + \sum_{j=1}^{n} E_{ij} = X_i \tag{5}$$

where $\mathbf{C}$ is the electricity consumption array, E_{ij} represents electricity transfer from node i to node j, and $\mathbf{X}$ is defined here as the total electricity flow array for each of the n nodes.

The water consumption associated with $\mathbf{X}$ in Eqn. (5) can be written

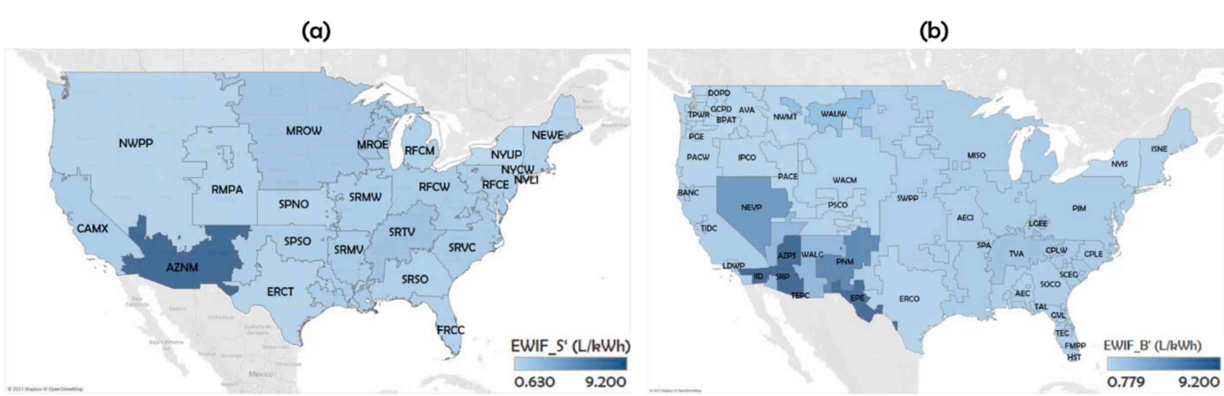

Fig. 2. (a). EPA eGRID subregional water intensity factor EWIF'$_S$ and (b). BA water intensity factor EWIF'$_B$.

as

$$w_i^X = w_i^G + \sum_{j=1, j\neq i}^{n} B_{ji} w_j^X \tag{6}$$

where w_i^X is the water consumption in all electricity flows through node i, and w_i^G represents the water consumed by electricity generation at node i. $\mathbf{B}$ is the direct outflow coefficient matrix and can be calculated as

$$\mathbf{B} = \widehat{\mathbf{X}}^{-1}\mathbf{E} = \begin{bmatrix} 0 & \frac{E_{12}}{X_1} & \cdots & \frac{E_{1n}}{X_1} \\ \frac{E_{21}}{X_2} & 0 & \ddots & \frac{E_{2n}}{X_2} \\ \vdots & \ddots & \ddots & \vdots \\ \frac{E_{n1}}{X_n} & \frac{E_{n2}}{X_n} & \cdots & 0 \end{bmatrix} \tag{7}$$

where $\widehat{\mathbf{X}}^{-1}$ is the diagonal matrix of $\mathbf{X}$, and the $(i,j)^{th}$ element B_{ij} represents the fraction of total electricity flows of node i that is exported to node j. By its definition, $B_{ij} = 0$ when $i = j$.

Eqn. (6) can be rearranged into matrix form:

$$\mathbf{w}^X = \mathbf{w}^G(\mathbf{I}-\mathbf{B})^{-1} = \mathbf{w}^G\mathbf{T} \tag{8}$$

where $\mathbf{T} = (\mathbf{I}-\mathbf{B})^{-1}$ is referred to as the total outflow coefficient matrix in input-output theory (Qu et al., 2017). Therefore, $\mathbf{T}$ captures all electricity transfers through infinite paths within the grid, and the element T_{ij} represents the proportion of aggregated electricity transfers to node j that is generated by node i.

This study extends the EEIO model by looking at the water scarcity at the origin of the water. To do so, "scarce" water consumption s_i is defined here to quantify the impacts of water consumption in region i. Akin to water consumption associated with total electricity flow (w_i^X), the "scarce" water consumption associated with $\mathbf{X}$ (s_i^X) can be written as

$$s_i^X = s_i^G + \sum_{j=1, j\neq i}^{n} B_{ji} s_j^X \tag{9}$$

In this study, the w_i^G and s_i^G are determined at the BA level using

$$w_i^G = \mathrm{EWIF}'_{B,i} G_i \tag{10}$$

$$s_i^G = w_i^G(\mathrm{AWARE-US\ CF})_i \tag{11}$$

where $\mathrm{EWIF'}_B$ is the BA-level water intensity derived from Eqn. (4), $(\mathrm{AWARE-US\,CF})_i$ is averaged over all counties in a BA, and G_i is the total electricity generation in BA i.

Examination of Eqn. (9) leads to determination of the scarce water consumption as

$$\mathbf{s}^X = \mathbf{s}^G\mathbf{T} \tag{12}$$

Furthermore, the EWIF for purchased electricity in each node can be determined as

$$\mathbf{EWIF_B} = \mathbf{w}^X\widehat{\mathbf{X}}^{-1} = \mathbf{w}^G\mathbf{T}\widehat{\mathbf{X}}^{-1} \tag{13}$$

Likewise, the scarce water index at the BA level ($\mathrm{SWI_B}$), which is the volume of scarce water per kWh of consumed electricity, is defined here to quantify the overall impacts of water consumption in each region on overall water availability. $\mathrm{SWI_B}$ can be calculated as

$$\mathbf{SWI_B} = \mathbf{s}^X\widehat{\mathbf{X}}^{-1} = \mathbf{s}^G\mathbf{T}\widehat{\mathbf{X}}^{-1} \tag{14}$$

In addition, all the water consumption due to electricity transfers through infinite paths from the power generating grid to the consuming grid can be traced using

$$\mathbf{T_w} = \widehat{\mathbf{w}^G}\mathbf{T}\mathbf{B}^C \tag{15}$$

where $\widehat{\mathbf{w}^G}$ is the matrix of diagonal components of $\mathbf{w}^G$. $\mathbf{B}^C$, which is a diagonal matrix that represents the fraction of electricity consumption in total electricity flow, is calculated as

$$\mathbf{B}^C = \widehat{\mathbf{C}}\widehat{\mathbf{X}}^{-1} \tag{16}$$

where $\widehat{\mathbf{C}}$ is the matrix of diagonal elements of $\mathbf{C}$. The $(i,j)^{th}$ element of $\mathbf{T_w}$ represents the total embodied water consumption transferred from generating grid i to consuming grid j. Likewise, the scarce water consumption due to electricity transfers can also be traced as

$$\mathbf{T_s} = \widehat{\mathbf{s}^G}\mathbf{T}\mathbf{B}^C \tag{17}$$

where $\widehat{\mathbf{s}^G}$ is the matrix of diagonal components of $\mathbf{s}^G$.

3. Results and case study

3.1. Results

Fig. 3 compares the water intensity factors with and without consideration of virtual water transfers at the BA-level. Results show that $\mathrm{EWIF'}_B$ varies from 0.779 to 9.200 L/kWh with an average of 2.340 L/kWh, whereas $\mathrm{EWIF_B}$ has a slightly smaller range (0.795 to 9.084 L/kWh) with an average of 2.251 L/kWh. The moderation of $\mathrm{EWIF_B}$ values is due to the mixing of electricity between both high and low $\mathrm{EWIF_B}$ regions. Specifically, water intensity factors of 11 BAs changed more than ±10% and those for 6 BAs changed over ±20%. The Arizona Public Service Company (AZPS), Imperial Irrigation District (IID) and Salt River Project Agricultural Improvement and Power District (SRP), three BAs located within or partially within subregion AZNM, have $\mathrm{EWIF_B}$ values over 20% below corresponding $\mathrm{EWIF'}_B$values due to heavy electricity imports from neighboring low water intensity regions. On the other hand, the water intensity factor of PacifiCorp East (PACE) increases from 1.10 L/kWh to 1.45 L/kWh (+27.6%) due to electricity imports from AZNM.

Fig. 4(a) shows AWARE-US CF values in the contiguous U.S. (Lee et al., 2019) EWIF and SWI values, which are uniformly distributed among counties within a BA, are presented in Fig. 4(b) and Fig. 4(c), respectively. The map reveals that counties in Central and Southwestern areas experience the worst water shortage and therefore have the highest AWARE-US CF values in the country. Eastern regions, however, show small AWARE-US CF values, indicating more abundant water resources.

Fig. 4(b) shows that areas of Arizona, New Mexico, Nevada, and western Texas have the highest EWIF, demonstrating the significance of evaporation from reservoir associated hydropower plants. Grubert (Grubert, 2016) found that hydropower has a broader range of possible water intensity factors than other power generation sources because of the variation in local climate and native plants. On the contrast, low water intensities can be achieved when reservoirs replace water intensive land cover like wetlands, as seen in Northwestern and Northeastern areas.

The calculated SWI are shown in Fig. 4(c). Counties that appear dark orange are those where consuming large amounts of electricity has a high impact on regional water availability. The map shows that areas in the Southwest (especially Arizona, western Texas, New Mexico, and Oklahoma) have the highest SWI.

Fig. 5 shows the percentile distribution of SWI values per county. It is assumed that the SWI of BA is uniformly distributed to all counties within the same BA. Results reveal that the SWI of counties in the Southwest and North Central regions correspond to the 90th percentile or more, indicating that consuming large amounts of water in these regions has the largest impact on regional water availability. Results also show that counties in the Northwest and Midwest regions are positioned within the 50th to 90th percentile, indicating medium impacts on

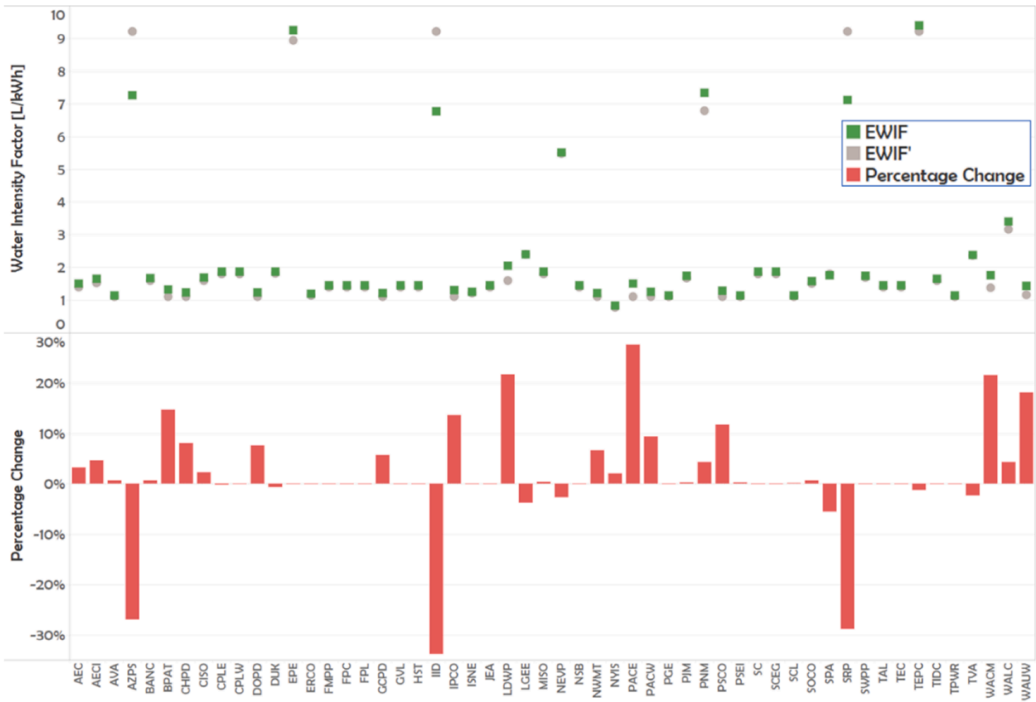

Fig. 3. Comparison of water intensity factor at the BA-level. Gray circles and green squares in the figure represent $EWIF'_B$ and $EWIF_B$, respectively. The bar chart below reveals the percentage change in the water intensity factors after incorporating electricity and water flows.

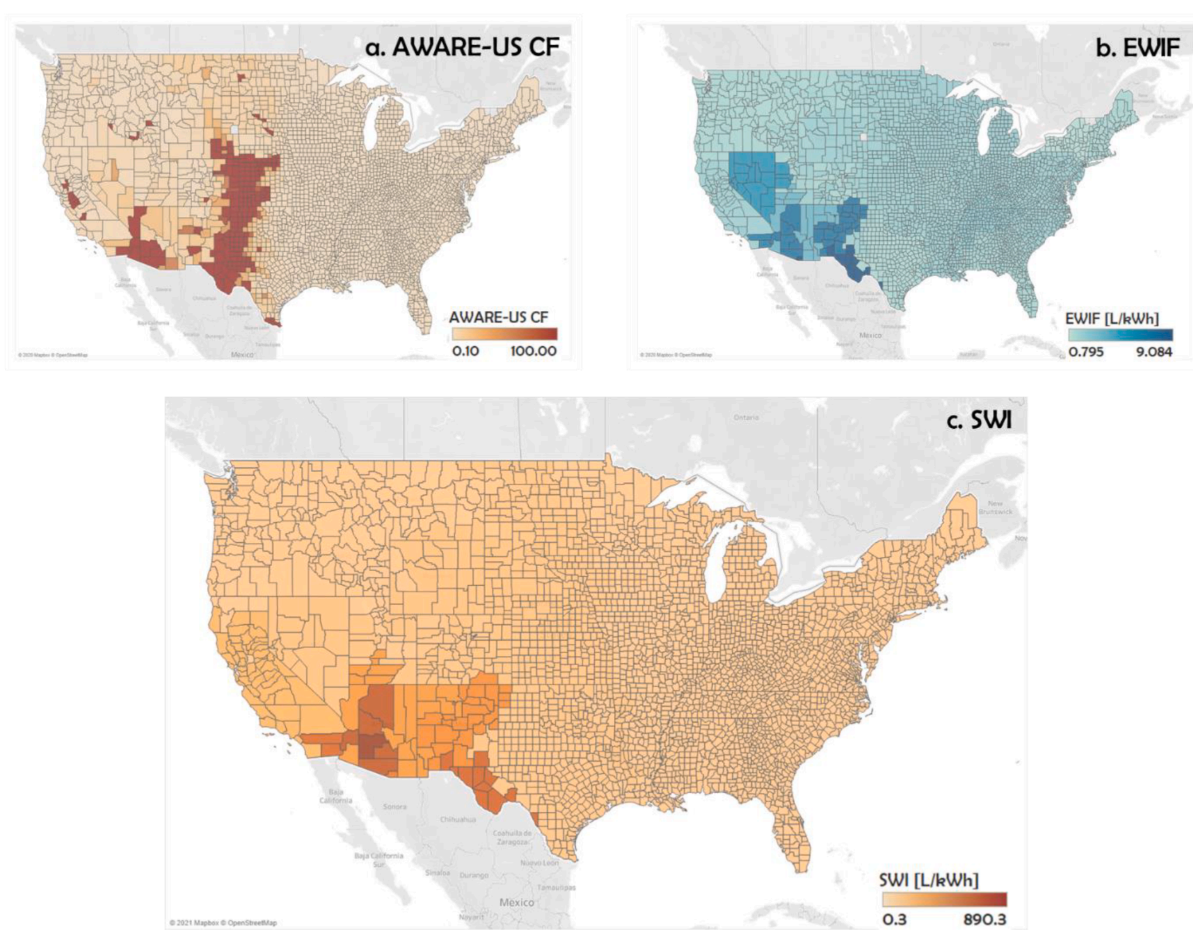

Fig. 4. U.S. map of environmental metrics (Chen and Wemhoff, 2021a) (a). AWARE-US CF (reproduced image using published data) (Lee et al., 2019) (b). EWIF and (c). SWI.

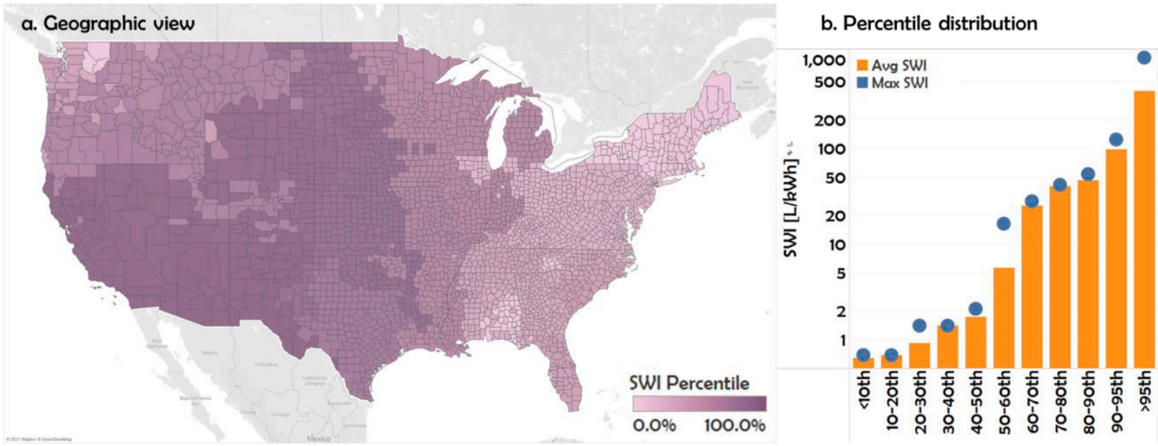

Fig. 5. Percentile distribution of SWI values at county-level (a). geographic view, (b). detailed percentile distribution and maximum SWI of each percentile range.

regional water scarcity from consuming water. Negligible impacts are found in the Northeast due to low EWIF values and sufficient water resources. The value of SWI grows rapidly with percentile range above the 80th percentile.

Fig. 6 compares three metrics: AWARE-US CF (Fig. 6(a)), EWIF (Fig. 6(b)) and SWI (Fig. 6(c)) using the state of Arizona as an example. Fig. 6(a) shows that multiple counties in Arizona (e.g., Mohave, La Paz, and Yuma) have AWARE-US CF values capped at 100, indicating extreme water scarcity. Fig. 6(b) illustrates that Mohave and Yuma Counties have EWIF values of 3.293 L/kWh, which is 53% less than La Paz County, which possesses an EWIF of 7.014 L/kWh. This difference in EWIF is because Mohave and Yuma Counties are categorized within the Western Area Power Administration - Desert Southwest Region (WALC) BA, whose 70% of power generated in 2019 was from hydropower and pumped storage in southern Utah. Overall, Fig. 6(c) shows that Mohave and Yuma Counties have an SWI of 287.8 L/kWh, while La Paz County has an SWI of 678.0 L/kWh. The results illustrate that AWARE-US CF and EWIF (while incorporating electricity transfers) are essential in assessing regional water scarcity and water consumption individually, but SWI combines both water consumption and regional water scarcity to enable the minimization of impact on water availability by grid-based water consumption.

The largest water (**w**) and scarce water (**s**) transfers within the electric grid are shown in Fig. 7(a). Specifically, water transmissions of at least 10^7 m^3 and scarce water transmission at least 10^8 m^3 are included. Fig. 7(a) reveals that the Salt River Project Agricultural Improvement and Power District (SRP), which occupies 40.3% of total local water consumption for power generation, is the generating grid that transmitted the most water to other BAs in 2019. The two largest customers who received electricity from SRP are the California Independent System Operator (CISO) and the Arizona Public Service Company (AZPS). Interestingly, CISO is the BA that receives the most embedded water from other BAs due to large electricity imports. Fig. 7 (b) reveals that SRP is also the source of several of the largest scarce water transfers due to its severe water shortage (AWARE-US CF = 100). It is also found that PJM Interconnection, LLC (PJM) and New York Independent System Operator (NYIS) also receive significant amounts of scarce water from SRP due to their large amounts of electricity imports although neither of them have direct electricity transfers with SRP, illustrating the complexity of the electric grid.

3.2. *Data center water scarcity footprint – A case study*

Bashroush and Lawrence (Bashroush and Lawrence, 2020) suggested that data centers may consume up to 500 TWh of electricity annually, which accounts for 3–4% of global electricity demand. The growth in the size and quantity of data centers increases concerns about the sector's growing energy usage and environmental impact. Therefore, a case study is performed that predicts and analyzes data center WSF values to demonstrate the concepts and methods proposed in this study.

Eqn. (3) indicates that WSF depends on the location-specific quantities AWARE-US CF and SWI as well as site water consumption (W_{site})

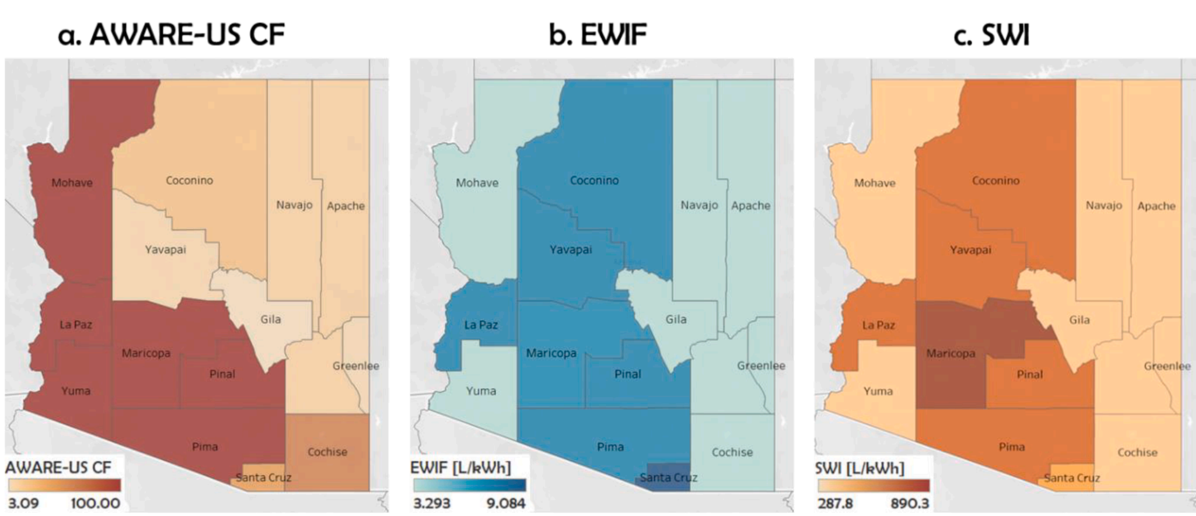

Fig. 6. County-level environmental metrics for state of Arizona (a). AWARE-US CF, (b). EWIF and (c). SWI.

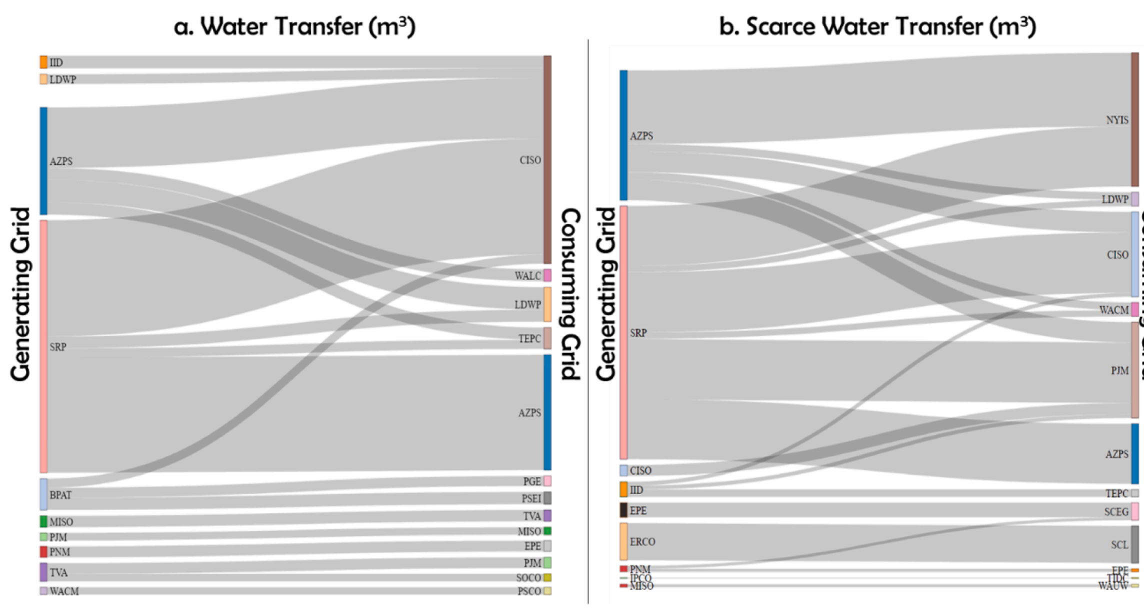

Fig. 7. Embodied water and scarce water transfer within the electric grid: (a) Water transfers $\geq 10^7$ m^3 (b) Scarce water transfers $\geq 10^8$ m^3.

and site power consumption (P_{site}). However, site-based data are difficult to obtain. Facebook is one of the few companies that provide environmental impact of their data centers through two annualized data center performance metrics: power usage effectiveness (PUE) and water usage effectiveness (WUE), which are provided as a combined metric for all sites in 2020 (*Facebook Sustainability*, 2021). PUE is a widely-used data center energy efficiency metric defined as the ratio of to data center IT equipment energy consumption (P_{IT}). WUE, on the other hand, measures the direct water use for data center operation and is calculated as the ratio of W_{site} to P_{IT}. Therefore, the ratio of WSF to P_{IT} of eight Facebook data centers located in the contiguous U.S. are determined here to demonstrate the usefulness of the WSF metric:

$$\frac{WSF}{P_{IT}} = (\mathrm{AWARE-US\ CF})(\mathrm{WUE}) + (\mathrm{SWI})(\mathrm{PUE}) \quad (18)$$

As PUE and WUE are found to be the annual average of all sites, they are applied to all data centers listed in Table 1. Eqn. (18) therefore indicates that location-specific metrics SWI and AWARE-US CF enable the comparison of WSF for identical data centers at various locations.

Table 1 provides the AWARE-US CF and SWI for selected Facebook data center locations and the resultant ratio of WSF to P_{IT}. Results show a broad range of WSF/P_{IT} that varies from 0.83 to 426 L/kWh, which emphasizes that an identical data center built in different regions could have dramatically different water stress impacts. Specifically, the data center constructed in Forest City, NC yields the lowest WSF /P_{IT} due to sufficient water resources and a low SWI, whereas the same data center built in Los Lunas, NM leads to much higher WSF/P_{IT} due to its higher water scarcity and SWI. A 1 MW hyperscale data center built in both Forest City, NC has a WSF less than 1/500th of an identical data center for Los Lunas, NM, and the Forest City, NC data center saves over 100 L/s of scarce water compared its Los Lunas, NM counterpart, which illustrates the dependence of facility location on holistic water stress impact.

Table 1
WSF/P_{IT} Prediction for Facebook data centers (WUE = 0.30 L/kWh, PUE = 1.10).

Facebook Data Center Site	AWARE-US CF	SWI (L/kWh)	$\frac{WSF}{P_{IT}}$ (L/kWh)
Altoona, IA	0.76	40.56	44.84
Forest City, NC	0.36	0.66	0.83
Fort Worth, TX	2.31	25.29	28.51
New Albany, OH	0.49	0.69	0.90
Papillion, NE	8.45	40.56	47.15
Prineville, OR	2.19	2.87	3.82
Henrico, VA	0.45	0.69	0.89
Los Lunas, NM	100.00	359.70	425.67

4. Discussion

4.1. Data limitations and uncertainties

Although this study reveals the importance of virtual water transfer accounting in water stress impact analysis and discloses the relationships between direct/indirect water scarcity and the water scarcity footprint of electricity consuming facilities, there are certain data limitations that bring uncertainties into the results. First, the electricity transfers among BAs are presented on an annual basis, and better spatial and temporal resolutions of data could lead to more robust analysis. Second, the aggregated electricity data is gathered from self-reporting, which leads to inevitable uncertainties even though they are currently the best available and widely used in tracking materials embodied in electricity related research (Chini et al., 2018; de Chalendar et al., 2019; Qu et al., 2017). For example, there were eight registered international BAs in 2019, while only five reported electricity transfers consistently. Third, this study quantifies the electricity consuming facility water stress impact by incorporating the location and fuel type specific water intensities. However, due to the coarseness of data, interpolating BA level water intensity from the eGRID subregion level causes unavoidable uncertainties. Finally, this study incorporates the up-to-date and best-guess assessments of water consumption for energy systems in the U.S. (Peer et al., 2019). However, an accurate quantitative uncertainty estimate is not possible due to major data limitations. Generally, water consumption is barely measured, traced or published. Therefore, the data used to estimate energy water intensity is a combination of empirical, self-reported and derived values based upon physical relationships. Furthermore, those values are conservatively overestimated by assuming water quality is fresh when it is not known (Peer et al., 2019).

4.2. Sustainable water management

Water resources are essential for life to exist. However, severe water shortages exist in many regions. At least 1 billion people worldwide lack access to water, and a total of 2.7 billion people find water to be scarce for at least one month of the year (*Water Scarcity*, 2021). Therefore, it is necessary to use water responsibly now. First, it is important to develop technologies and policies that aim at sustainable water management, especially in water scarce regions. In Arizona, 84% of the state has severe drought conditions (i.e., the highest AWARE-US CF) and is preparing for its first ever Tier 1 water shortage cut, which will force the state to decrease the water draw from the Colorado River (Blufish, 2021). The burden of water conservation mainly falls on farmers since most of the water sourced from the river goes to the agriculture industry. However, hydropower should be avoided in this region, which consumes approximately 64,000 Liters of fresh water to produce 1,000 kWh of electricity due to limited landcover evapotranspiration and a high evaporation potential. Moreover, improvements in the distribution infrastructure can be extremely beneficial. An electricity consuming facility in a water-rich region may negatively impact water availability in a water-poor region by consuming electricity generated from that region. The SWI and WSF methodologies proposed in this study could be used to optimize the distribution infrastructure in a way that minimizes the water stress impact in different regions since it incorporates the effects of water availability into power generation processes and the predicted electricity flows.

5. Conclusion

This study improves the quantification of electricity consuming facility indirect water consumption by tracking virtual water transfers at a finer spatial resolution (i.e., BA level) within the U.S. electric grid. Specifically, EWIF values are updated from a consumer's point of view that includes the virtual water transfers associated with electricity exchanges across regional boundaries. These updated EWIF values show a smaller range (0.795 to 9.084 L/kWh) compared to the range of values that exclude electricity exchanges (EWIF', 0.779 to 9.200 L/kWh).

This study also fulfills electricity consumer WSF predictions by quantifying indirect water consumption impact using the proposed SWI metric. The tracking of scarce water through the U.S. electric grid at the BA level offers a spatially robust model that enables an improved accounting of water scarcity and water resources' location for water stress impact prediction. The results reveal that the largest burden for local water availability occurs for power generation that consumes large amounts of water in western Texas and Arizona, with significant effects also associated with power generation in Central states such as Nebraska, Kansas and Oklahoma. Results also show that SRP is one of the largest water and scarce water providers to other BAs, which spotlights the significant contribution of electricity importing from water scarce regions to water stress impact.

Moreover, a case study that examines the WSF of extensive electricity consuming facilities (i.e., data centers) is presented. It reveals that the water stress impact of a data center built in one location could be significantly higher than another, although both data centers consumed exact same amount of power and on-site water. Therefore, this study once again highlights the potential strategies to reduce the impact of water consumption on regional water availability, and that these strategies should account for virtual water transfers within the electric grid. Furthermore, this study also serves as a foundation to inform decision makers that shifting the burden of water scarcity and reducing the water stress impact are urgently needed, especially in water scarce regions.

Future work should examine the use of these metrics for guiding electricity consuming facility siting decisions that enhance water sustainability and management. This type of analysis can be easily extended to all other buildings that consume large amounts of water and electricity such as factories. These studies would investigate the balance between large on-site water consuming cooling systems (e.g., evaporative cooling) versus systems with higher electrical consumption and lower on-site water consumption such as the conventional use of direct expansion air conditioning units.

CRediT author statement

Assessing Indirect Water Use and Water Scarcity Footprint by Buildings in the United States.**Li Chen**: Methodology, Formal analysis, Investigation, Writing – Original draft preparation, Visualization.**Aaron P**. Wemhoff: Funding, Conceptualization, Writing – Reviewing and editing, Supervision

Declaration of Competing Interest

The authors declare that they have no known competing financial interests or personal relationships that could have appeared to influence the work reported in this paper. The authors declare the following financial interests/personal relationships which may be considered as potential competing interests:

Acknowledgments

Preliminary work by Tao Dai (Villanova University) is appreciated. This material is based upon work supported by the National Science Foundation (NSF) under Grant No. IIP 1738782. Any opinions, findings, and conclusions or recommendations expressed in this material are those of the author(s) and do not necessarily reflect the views of the National Science Foundation.

References

Arpke, A., Hutzler, N., 2005. Operational life-cycle assessment and life-cycle cost analysis for water use in multioccupant buildings. J. Archit. Eng. 11 (3), 99–109, 10.1061/(ASCE)1076-0431(2005)11:3(99).
Bardhan, S., Choudhuri, I.R., 2016. Studies on virtual water content of Urban buildings in India. Indian J. Sci. Technol. 9 (6) https://doi.org/10.17485/ijst/2016/v9i6/87671.
Bartos, M.D., Chester, M.V., 2014. *The conservation nexus: valuing interdependent water and energy savings in Arizona* (world) [Research-article]. ACS Publications; Am. Chem. Soc. https://doi.org/10.1021/es4033343.
Bashroush, R., Lawrence, A., 2020. Beyond PUE. Tackling IT's wasted terawatts 4.
Blufish, 2021. What the deepening water shortage means for Arizona homeowners. AZ Big Media https://azbigmedia.com/real-estate/residential-real-estate/what-the-deepening-water-shortage-means-for-arizona-homeowners/.
Boulay, A.-M., Bare, J., Benini, L., Berger, M., Lathuillière, M.J., Manzardo, A., Margni, M., Motoshita, M., Núñez, M., Pastor, A.V., Ridoutt, B., Oki, T., Worbe, S., Pfister, S., 2018. The WULCA consensus characterization model for water scarcity footprints: assessing impacts of water consumption based on available water remaining (AWARE). Int. J. Life Cycle Assess. 23 (2), 368–378. https://doi.org/10.1007/s11367-017-1333-8.
Chapagain, A.K., & Hoekstra, A.Y. (2008). The global component of freshwater demand and supply: an assessment of virtual water flows between nations as a result of trade in agricultural and industrial products. Water Int., 33(1), 19–32. 10.1080/02508060801927812.
Chen, L., & Wemhoff, A.P. (2021a). *Supplementary information for assessing the impact of electricity consumption on water resources in the U.S., Mendeley Data*. https://data.mendeley.com/drafts/hb66dknt5t.
Chen, L., Wemhoff, A.P., 2021b. Predicting embodied carbon emissions from purchased electricity for United States counties. Appl. Energy 292, 116898. https://doi.org/10.1016/j.apenergy.2021.116898.
Chini, C.M., Djehdian, L.A., Lubega, W.N., Stillwell, A.S., 2018. Virtual water transfers of the US electric grid. Nature Energy 3 (12), 1115–1123. https://doi.org/10.1038/s41560-018-0266-1.
Cohen, E., Ramaswami, A., 2014. The water withdrawal footprint of energy supply to cities. J. Ind. Ecol. 18 (1), 26–39. https://doi.org/10.1111/jiec.12086.
Crawford, R.H., Pullen, S., 2011. Life cycle water analysis of a residential building and its occupants. Build. Res. Inf. 39 (6), 589–602. https://doi.org/10.1080/09613218.2011.584212.
Dang, Q., Lin, X., Konar, M., 2015. Agricultural virtual water flows within the United States. Water Resour. Res. 51 (2), 973–986. https://doi.org/10.1002/2014WR015919.
de Chalendar, J.A., Taggart, J., & Benson, S.M. (2019). Tracking emissions in the US electricity system. *Proc. Natl. Acad. Sci.*, 116(51), 25497–25502. 10.1073/pnas.1912950116.
Facebook Sustainability. (2021). Facebook Sustainability. https://sustainability.fb.com/.

Frischknecht, R., Fantke, P., Tschümperlin, L., Niero, M., Antón, A., Bare, J., Boulay, A.-. M., Cherubini, F., Hauschild, M.Z., Henderson, A., Levasseur, A., McKone, T.E., Michelsen, O.i, Canals, L.M., Pfister, S., Ridoutt, B., Rosenbaum, R.K., Verones, F., Vigon, B., Jolliet, O., 2016. Global guidance on environmental life cycle impact assessment indicators: progress and case study. Int. J. Life Cycle Assess. 21 (3), 429–442. https://doi.org/10.1007/s11367-015-1025-1.

Garcia, S., Rushforth, R., Ruddell, B.L., Mejia, A., 2020. Full domestic supply chains of blue virtual water flows estimated for major U.S. Cities. Water Resour. Res. 56 (4) https://doi.org/10.1029/2019WR026190.

Grubert, E.A., 2016. Water consumption from hydroelectricity in the United States. Adv. Water Resour. 96, 88–94. https://doi.org/10.1016/j.advwatres.2016.07.004.

HIFLD Open Data. (2020). https://hifld-geoplatform.opendata.arcgis.com/.

ISO 14046:2014. (2014). https://www.iso.org/cms/render/live/en/sites/isoorg/contents/data/standard/04/32/43263.html.

Jones, E., van Vliet, M.T.H., 2018. Drought impacts on river salinity in the southern US: implications for water scarcity. Sci. Total Environ. 644, 844–853. https://doi.org/10.1016/j.scitotenv.2018.06.373.

Kodra, E., Sheldon, S., Dolen, R., Zik, O., 2015. The North american electric grid as an exchange network: an approach for evaluating energy resource composition and greenhouse gas mitigation. Environ. Sci. Technol. 49 (22), 13692–13698. https://doi.org/10.1021/acs.est.5b03015.

Lee, J., Lee, M., Chun, Y.-.Y., Lee, K., 2018. Uncertainty analysis of the water scarcity footprint based on the AWARE model considering temporal variations. Water (Basel) 10 (3), 341. https://doi.org/10.3390/w10030341.

Lee, U., Xu, H., Daystar, J., Elgowainy, A., Wang, M., 2019. AWARE-US: quantifying water stress impacts of energy systems in the United States. Sci. Total Environ. 648, 1313–1322. https://doi.org/10.1016/j.scitotenv.2018.08.250.

Liao, X., Zhao, X., Hall, J.W., Guan, D., 2018. Categorising virtual water transfers through China's electric power sector. Appl. Energy 226, 252–260. https://doi.org/10.1016/j.apenergy.2018.05.132.

Liao, X., Zhao, X., Liu, W., Li, R., Wang, X., Wang, W., Tillotson, M.R., 2020. Comparing water footprint and water scarcity footprint of energy demand in China's six megacities. Appl. Energy 269, 115137. https://doi.org/10.1016/j.apenergy.2020.115137.

Liu, J., Yang, H., Gosling, S.N., Kummu, M., Flörke, M., Pfister, S., Hanasaki, N., Wada, Y., Zhang, X., Zheng, C., Alcamo, J., Oki, T., 2017. Water scarcity assessments in the past, present, and future. Earth's Future 5 (6), 545–559. https://doi.org/10.1002/2016EF000518.

Macknick, J., Newmark, R., Heath, G., Hallett, K.C., 2012. Operational water consumption and withdrawal factors for electricity generating technologies: a review of existing literature. Environ. Res. Lett. 7 (4), 045802 https://doi.org/10.1088/1748-9326/7/4/045802.

Maps—EIA. (2020). Layer information for interactive state maps. https://www.eia.gov/maps/layer_info-m.php.

Meng, J., Chen, G.Q., Shao, L., Li, J.S., Tang, H.S., Hayat, T., Alsaedi, A., Alsaadi, F., 2014. Virtual water accounting for building: case study for E-town, Beijing. J. Clean. Prod. 68, 7–15. https://doi.org/10.1016/j.jclepro.2013.12.045.

Meng, M., Grubert, E., Peer, R.A.M., Sanders, K.T., 2020. Spatially allocating life cycle water use for us coal-fired electricity across producers, generators, and consumers. Energy Technol. 8 (11), 1901497 https://doi.org/10.1002/ente.201901497.

Mubako, S.T., & Lant, C.L. (2013). Agricultural virtual water trade and water footprint of U.S. states. annals of the association of American geographers, 103(2), 385–396. 10.1080/00045608.2013.756267.

Peer, R.A.M., Grubert, E., Sanders, K.T., 2019. A regional assessment of the water embedded in the US electricity system. Environ. Res. Lett. 14 (8), 084014 https://doi.org/10.1088/1748-9326/ab2daa.

Peer, R.A.M., Sanders, K.T., 2018. The water consequences of a transitioning US power sector. Appl. Energy 210, 613–622. https://doi.org/10.1016/j.apenergy.2017.08.021.

Proença, L.C., Ghisi, E., 2010. Water end-uses in Brazilian office buildings. Resour. Conserv. Recycl. 54 (8), 489–500. https://doi.org/10.1016/j.resconrec.2009.10.005.

Qu, S., Wang, H., Liang, S., Shapiro, A.M., Suh, S., Sheldon, S., Zik, O., Fang, H., Xu, M., 2017. A quasi-input-output model to improve the estimation of emission factors for purchased electricity from interconnected grids. Appl. Energy 200, 249–259. https://doi.org/10.1016/j.apenergy.2017.05.046.

Real-time Operating Grid. (2020). U.S. energy information administration (EIA). https://www.eia.gov/electricity/gridmonitor/index.php.

Ridoutt, B.G., Pfister, S., 2010. A revised approach to water footprinting to make transparent the impacts of consumption and production on global freshwater scarcity. Global Environ. Change 20 (1), 113–120. https://doi.org/10.1016/j.gloenvcha.2009.08.003.

Rijsberman, F.R., 2006. Water scarcity: fact or fiction? Agric. Water Manag. 80 (1), 5–22. https://doi.org/10.1016/j.agwat.2005.07.001.

Rushforth, R.R., Ruddell, B.L., 2016. The vulnerability and resilience of a city's water footprint: the case of Flagstaff, Arizona, USA. Water Resour. Res. 52 (4), 2698–2714. https://doi.org/10.1002/2015WR018006.

Sanders, K.T., 2014. *Critical review: uncharted waters? the future of the electricity-water nexus* (world) [review-article]. ACS publications. Am. Chem. Soc. https://doi.org/10.1021/es504293b.

Schyns, J.F., Hoekstra, A.Y., Booij, M.J., 2015. Review and classification of indicators of green water availability and scarcity. Hydrol. Earth Syst. Sci. 19 (11), 4581–4608. https://doi.org/10.5194/hess-19-4581-2015.

US EIA. (2021). *Use of electricity*. https://www.eia.gov/energyexplained/electricity/use-of-electricity.php.

US EPA, O., 2015a. *Emissions & generation resource integrated database (eGRID)* [data and tools]. US EPA https://www.epa.gov/energy/emissions-generation-resource-integrated-database-egrid.

US EPA, O., 2015b. *Download the eGRID2016 Shapefiles* [Data and Tools]. US EPA https://www.epa.gov/energy/download-egrid2016-shapefiles.

Wang, R., Zimmerman, J.B., Wang, C., Font Vivanco, D., Hertwich, E.G, 2017. Freshwater vulnerability beyond local water stress: heterogeneous effects of water-electricity nexus across the continental United States. Environ. Sci. Technol. 51 (17), 9899–9910. https://doi.org/10.1021/acs.est.7b01942.

WaterScarcity. (2021). World wildlife fund. https://www.worldwildlife.org/threats/water-scarcity.

Willis, R.M., Stewart, R.A., Giurco, D.P., Talebpour, M.R., Mousavinejad, A., 2013. End use water consumption in households: impact of socio-demographic factors and efficient devices. J. Clean. Prod. 60, 107–115. https://doi.org/10.1016/j.jclepro.2011.08.006.

Xie, X., Jiang, X., Zhang, T., Huang, Z., 2020. Study on impact of electricity production on regional water resource in China by water footprint. Renew. Energy 152, 165–178. https://doi.org/10.1016/j.renene.2020.01.025.

Zhang, C., Zhong, L., Liang, S., Sanders, K.T., Wang, J., Xu, M., 2017. Virtual scarce water embodied in inter-provincial electricity transmission in China. Appl. Energy 187, 438–448. https://doi.org/10.1016/j.apenergy.2016.11.052.

Zhang, J.C., Zhong, R., Zhao, P., Zhang, H.W., Wang, Y., Mao, G.Z., 2016. International energy trade impacts on water resource crises: an embodied water flows perspective. Environ. Res. Lett. 11 (7), 074023 https://doi.org/10.1088/1748-9326/11/7/074023.

Zhao, X., Li, Y.P., Yang, H., Liu, W.F., Tillotson, M.R., Guan, D., Yi, Y., Wang, H., 2018. Measuring scarce water saving from interregional virtual water flows in China. Environ. Res. Lett. 13 (5), 054012 https://doi.org/10.1088/1748-9326/aaba49.

Zheng, X., Wang, C., Cai, W., Kummu, M., Varis, O., 2016. The vulnerability of thermoelectric power generation to water scarcity in China: current status and future scenarios for power planning and climate change. Appl. Energy 171, 444–455. https://doi.org/10.1016/j.apenergy.2016.03.040.